Displacement-Based Seismic Assessment of Low-Height Confined Masonry Buildings

Amador Terán-Gilmore,[a] Oscar Zuñiga-Cuevas,[a] and Jorge Ruiz-García[b]

This paper presents a practical displacement-based evaluation procedure for the seismic assessment of low-height regular confined masonry buildings. First, the so-called Coefficient Method established in several FEMA documents is adapted to obtain rapid estimates of inelastic roof displacement demands for regular confined masonry buildings. For that purpose, a statistical study of constant relative strength inelastic displacement ratios of single-degree-of-freedom systems representing confined masonry buildings is carried out. Second, a nonlinear simplified model is introduced to perform pushover analysis of regular confined masonry buildings whose global and local behavior is dominated by shear deformations in the masonry walls. The model, which can be applied through the use of commercial software, can be used to establish the capacity curve of such buildings. Finally, the evaluation procedure is applied to a three-story building tested at a shaking table testing facility. [DOI: 10.1193/1.3111149]

INTRODUCTION

Displacement-based procedures for the seismic evaluation of existing structures and for the preliminary design of new structures are increasing in popularity. The practical objective of a displacement-based procedure is to predict the expected performance of a structure in future earthquake shaking. For this purpose, performance-based formats characterize performance in terms of damage to structural and nonstructural components. Since structural damage implies inelastic behavior, evaluation procedures require nonlinear analysis techniques to estimate the magnitude of inelastic deformation demands. Subsequently these demands are used to determine performance based on previously established acceptance criteria. Thus, the application of the concept of performance-based design and evaluation can only be successful in reducing seismic risk if nonlinear analysis techniques are applied in an extensive manner to existing and new construction.

According to its 2000 census, Mexico has close to 22 million housing units that house about 100 million people. Eighty percent of these dwellings are built with some type of masonry (unreinforced masonry or confined masonry with tie-end lightly-

[a] Universidad Autónoma Metropolitana, Depto. de Materiales, Av. San Pablo 180, 02200 México, D.F., México; tga@correo.azc.uam.mx
[b] Universidad Michoacana de San Nicolás de Hidalgo, Facultad de Ingeniería Civil, Edificio C, Cd. Universitaria, 58040 Morelia, México; jruizgar@stanfordalumni.org

Earthquake Spectra, Volume 25, No. 2, pages 439–464, May 2009; © 2009, Earthquake Engineering Research Institute

reinforced small-section columns and beams that surround brick masonry walls which might include or not include additional horizontal steel reinforcement placed into the mortar joints), and a large percent of those dwellings located close to seismic sources have not fared well during severe ground shaking. For instance, 25,353 units out of a sample of 140,572 were damaged during the 2003 Tecoman Earthquake (M_W=7.4), resulting in direct and indirect economical losses of about 123 million dollars (EERI 2006). Other examples of the high vulnerability of unreinforced and confined masonry dwellings and buildings in Mexico and other Latin-American countries have been reported by Ruiz-García et al. (2003) and Rodríguez (2005). Thus, seismic assessment procedures to evaluate the vulnerability of masonry construction are highly valuable.

Modern performance-based seismic assessment procedures for existing structures are based on: a) the evaluation of the structure-specific lateral deformation capacity, and b) the earthquake-induced displacement demand. Several proposals to move from force-based to displacement-based assessment methodologies have been made. Among them are the linear and nonlinear static procedures (LSP and NSP, respectively) discussed in *FEMA 273/274* (1997), *FEMA 306* (1999), *FEMA 356* (2000) and *FEMA 440* (2005). Although some of the displacement-based procedures proposed recently have specifically targeted masonry structures (e.g., Calvi 1999, Rodríguez 2005), there is still the need to formulate and calibrate simplified displacement-based procedures for the structural design and assessment of masonry buildings, and for estimating the seismic risk and developing earthquake loss estimation scenarios for a masonry building stock.

This paper introduces a practical displacement-based evaluation procedure that targets low-height confined masonry (CM) buildings. First, a simplified procedure to obtain estimates of inelastic roof displacement demands for regular CM buildings is adapted after the Coefficient Method established in several FEMA documents (e.g., *FEMA 273/274* 1997, *FEMA 306* 1999, *FEMA 356* 2000, *FEMA 440* 2005). In addition, a nonlinear simplified model is introduced to perform pushover analysis of regular CM buildings whose global and local behavior is dominated by shear deformations in the masonry walls. The model, which can be applied through the use of commercial software that has been readily available for many years, can be used to estimate the capacity curve of a CM building. Although the evaluation procedure can be applied to any type of masonry construction, the scope of the paper is limited to confined hand-made clay brick masonry walls, typically used in Latin-America and other regions of the world to build low-height housing units.

BASIS FOR A DISPLACEMENT-BASED APPROACH OF CM BUILDINGS

Based on ample experimental evidence derived from CM walls tested under in-plane lateral cyclic loading, Ruiz-García and Alcocer (1998) established a relationship between an increase in lateral drift, the evolution of damage, and structure degradation on CM walls. This relationship is schematically illustrated in Figure 1 and summarized in Table 1. K_o and K represent the initial lateral elastic stiffness and the lateral stiffness associated to a particular value of inter-story drift (D), respectively; and V_{max} and V the maximum shear and the shear associated to a particular value of D, respectively. As suggested in Table 1, it is common practice to normalize the stiffness corresponding to a

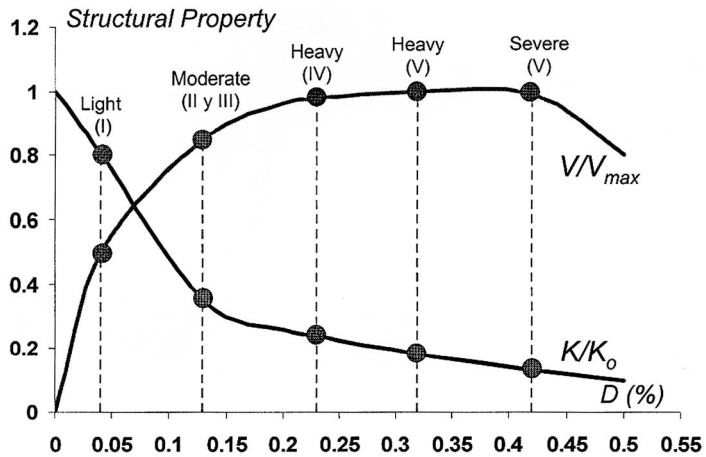

Figure 1. Evolution of damage and structural degradation on confined masonry walls (after Ruiz-García and Alcocer 1998).

certain level of inelastic behavior by the initial lateral elastic stiffness of the wall. Thus, by using the information included in Table 1, it is possible to formulate displacement-based evaluation procedures for low-height CM buildings. Particularly, limiting the peak lateral deformation demand under earthquake excitation within the lateral deformation

Table 1. Damage and degradation of confined masonry walls (after Ruiz-García and Alcocer 1998)

Observed damage	D (%)	K/K_o	V/V_{max}	Level of Damage
Flexural hairline horizontal cracking; hairline vertical cracking near the tie-end RC columns	0.04	0.8	0.5	Light (I)
First diagonal cracking due to diagonal tension in the masonry wall surface	0.13	0.35	0.85	Moderate (II and III)
Beginning of the inclined diagonal cracking at the ends of the tie-end columns	0.20	0.27	0.90	Heavy (IV)
Fully formed "X-shape" cracking on the masonry wall surface	0.23	0.24	0.98	Heavy (IV)
Concrete crushing; horizontal cracking spread over the tie-end column height	0.32	0.18	1.0	Heavy (V)
Concentrated diagonal cracking at the end of tie-end columns; concrete spalling in the tie-end columns	0.42	0.13	0.99	Severe (V)
Progression of diagonal cracking into the tie-end columns leading to rebar kicking of the longitudinal steel	0.50	0.10	0.80	Severe (not classified)

Table 2. Parameters used by the Flores and Alcocer (1996) backbone curve

Shear	Inter-story drift
V_{cr}	$D_{cr}=\frac{V_{cr}}{K_o h}$
$V_{max}=1.25V_{cr}$	$D_{max}=0.003$
$V_u=0.8V_{cr}$	$D_u=0.005$

associated to the maximum lateral capacity seems fundamental to avoid in-cycle strength degradation which may lead to unstable behavior of CM buildings and increased uncertainty during the evaluation process.

In addition, Ruiz-García and Alcocer (1998) also proposed the following expression to estimate the level of stiffness degradation in CM walls as a function of their D demand:

$$\frac{K_i}{K_o}=\left(\frac{1}{1+5300(D_i-D_{cr})^{1.2}}\right) \tag{1}$$

where K_i is the lateral stiffness corresponding to inelastic inter-story drift demand D_i, and D_{cr} the inter-story drift corresponding to first diagonal cracking in the wall's surface. Note that D_i in Equation 1 has to be larger than D_{cr}.

The backbone curve of CM walls provides information that is fundamental for their structural assessment. As discussed in *FEMA 306* (1999) document, this curve corresponds to the envelope of the hysteresis loops obtained experimentally in walls subjected to in-plane cyclic loading. In the case of low-height CM walls, their behavior tends to be dominated by shear deformations in such manner that their hysteretic behavior is characterized by significant cyclic and in-cycle strength degradation. Flores and Alcocer (1996) proposed a tri-linear curve to characterize the backbone curve of CM walls. While Table 2 indicates how the six parameters that define the Flores and Alcocer (1996) curve are estimated, Figure 2 depicts their model. V_{cr} corresponds to the design shear strength of the wall established according to the Masonry Technical Requirements of the 2004 edition of the Mexico City Building Code (MCBC 2004), h is the height of the wall; D_{max} is the drift at which V_{max} is reached; D_u corresponds to the ultimate drift achieved by the wall; and V_u is the shear force at ultimate.

The damage thresholds and descriptions, and the structural degradation levels implied by Figure 1 and Table 1 have been established specifically for CM structures that have similar design and construction requirements as those specified in the Masonry Technical Requirements of the MCBC (2004). This means that assessment of structures designed according to standards that imply a different level of confinement for the masonry or different mechanical characteristics for the masonry units and mortar require the development of specific damage thresholds. The recommendations also ignore rel-

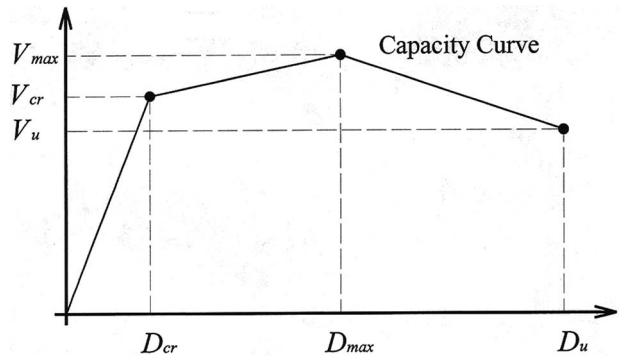

Figure 2. Idealized backbone curve for confined masonry walls (after Flores and Alcocer 1996).

evant geometrical characteristics of the walls, such as their aspect ratio. Because of this, the recommendations cannot be applied to individual walls, and are meant to describe a general state of damage and structural degradation in the critical story of a building.

WIDE-COLUMN MODEL FOR THE ELASTIC ANALYSIS OF CM BUILDINGS

In recent years, Mexican practicing engineers have widely used the *wide-column* model for the analysis and design of CM buildings. As shown in Figure 3, according to this model a multi-story CM building can be idealized as bare frames. Each wall is mod-

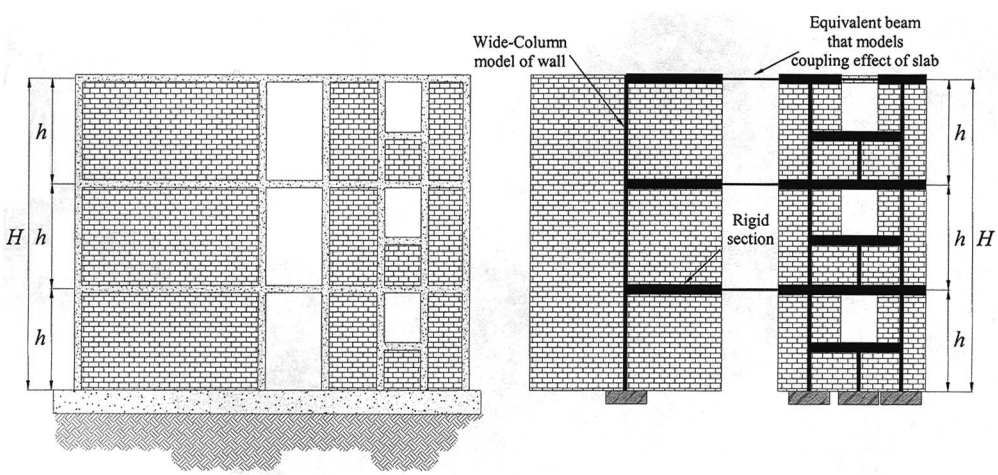

Figure 3. Elastic analysis technique for confined masonry buildings: a) confined masonry building, b) wide-column model of building.

Table 3. Experimental and analytical lateral stiffness of confined masonry specimens

Specimen	Experimental (KN/m) K_0 (+)	K_0 (−)	K_0 (Average)	Analytical (kN/m)
WW	111000	103000	107000	103000
WBW	86000	86000	86000	93000
WWW	126000	141000	133500	100000
3-D	112000	162000	137000	128000

eled as an equivalent column that concentrates its flexural and shear properties on its centerline. In addition, equivalent beams having a width estimated according to the Masonry Technical Requirements of the MCBC (2004), are used to model the coupling effect that the slab provides to the masonry walls. Note that equivalent-end beams having infinite stiffness both for flexure and shear are used to model the part of the slab that falls within the walls' length; and that short-walls due to openings are also modeled as wide-columns. It should be noted that this modeling technique has also been used in other Latin American countries (e.g., San Bartolome 1994).

The *wide-column* model has the potential to model the contributions of the masonry panel and of the confining tie-end reinforced concrete columns during the estimation of the mechanical properties of the CM wall. For that purpose, the modular ratio between the masonry and the concrete is used. In case the CM building is modeled as a planar frame, the analytical model of the in-plane walls should take into account the contribution of the out-of-plane walls that intersect them. A three-dimensional model allows a direct consideration of all walls as wide-columns. The elastic lateral stiffness of a wide-column can be estimated as follows:

$$K = \left[\frac{h^3}{\beta EI} + \frac{h}{GA_V} \right]^{-1} \tag{2}$$

where h is the height of the wall; A_V and I the shear area and moment of inertia of its cross section, respectively; E and G the masonry's modulus of elasticity and shear modulus, respectively; and β a factor that accounts for the end-fixity of the wall.

Through Equation 2, it is possible to take into account the wall's aspect ratio and its end-support conditions to establish the relative contribution of the flexural and shear lateral deformations to the lateral response of CM walls. Particularly, the lateral response of CM walls having both ends fixed and aspect ratios smaller than one is usually dominated by shear deformations. Independently of its aspect ratio, the effects of shear deformation tend to significantly increase relative to those associated to flexure as the level of damage increases in a CM wall (Zuñiga and Terán-Gilmore 2008).

Table 3 presents a comparison between the lateral stiffness obtained from the experimental response of three full-scale CM specimens (designated as *W-W*, *WBW*, *WWW*) and a full-scale two-story tri-dimensional specimen (designated as 3-D) tested under in-plane cyclic loading (Alcocer and Meli 1993, Ruiz-García 1995), and the corresponding

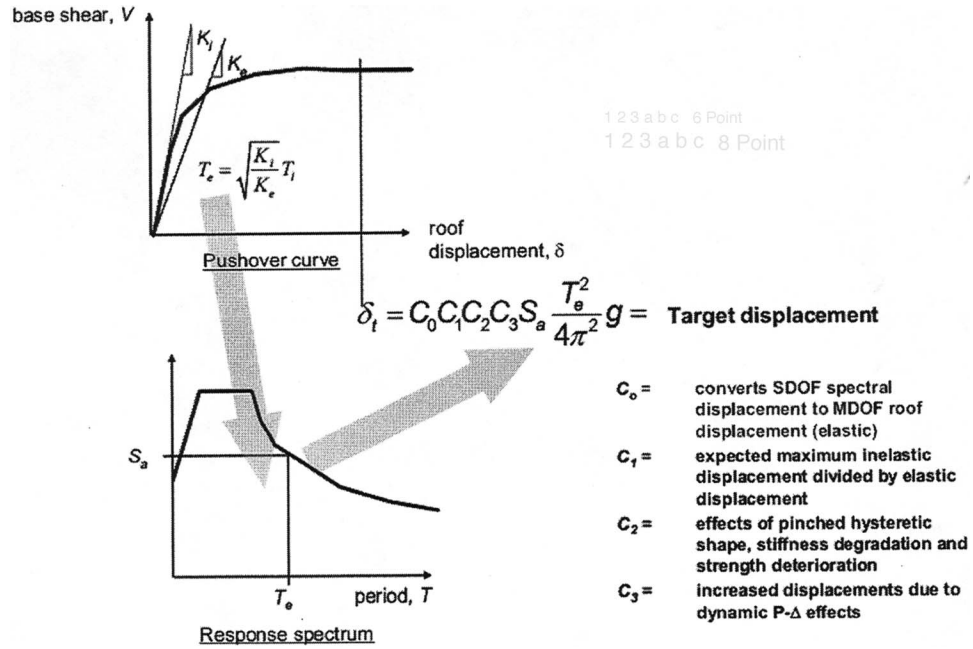

Figure 4. Coefficient Method procedure (after *FEMA 356* 2000).

stiffnesses computed from their corresponding *wide-column* model. As shown, Equation 2 provides a good estimation of the experimentally measured elastic lateral stiffness for all specimens. From the results presented in Table 3 and previous research observations (e.g., Bazán 1980, San Bartolome 1994), it can be concluded that the wide-column model is able to capture with reasonable approximation the elastic lateral stiffness of CM walls with different aspect-ratio and end-support conditions.

EVALUATION OF LATERAL DISPLACEMENT DEMANDS IN CM BUILDINGS

Nonlinear analysis procedures have been widely used by American practicing engineers since the publication of ATC-40 (1996), and FEMA-273/274 (1997). Particularly, the nonlinear static procedures (NSP) have become popular due to their simplicity and ability to provide useful insight regarding the expected performance of earthquake-resistant structures. Among the options available to estimate target displacement demands of existing structures is the so-called Coefficient Method, which is depicted in Figure 4. Recently, improvements to the Coefficient Method were proposed based on extensive analytical studies, which were reported in *FEMA 440* document (2005). Even though the Coefficient Method is aimed at estimating target displacements for reinforced concrete buildings, this approach can be adapted to estimate lateral displacement demands for CM buildings.

Table 4. Suggested values for C_0 after *FEMA 356* (2000)

	Performance Level		
Number of Stories	Immediate Operation	Life Safety	Collapse Prevention
1	1.0	1.0	1.0
2+	1.2	1.0	1.0

Field reconnaissance after earthquake events have consistently shown that severe structural damage tends to concentrate in the first story of CM structures. The stories above the first story tend to remain undamaged or with slight structural damage, even if the CM building has similar height-wise wall density (e.g., Ruiz-Garcia et al. 2003). This observation has been confirmed from experimental testing on small-scale and large-scale masonry specimens subjected to quasistatic cyclic or shaking-table testing (e.g., Ruiz-García 1995, Alcocer et al. 1996, Barragan and Alcocer 2006). Under these circumstances, the value of the coefficient C_0 involved in the Coefficient Method should be close, for low levels of damage, to the value indicated by the FEMA guidelines for shear buildings; and should tend to one as the level of damage in the building increases. Based on this, Table 4 summarizes suggested values of C_0 for the displacement-based assessment of CM buildings.

If as expected, low-height CM buildings do not exhibit significant P-Δ effects, coefficient C_3 could be neglected during the computation of the target displacement (δ_t). Thus, taking into account that the inelastic displacement ratio C_R can contemplate simultaneously the effects accounted for by parameters C_1 and C_2 (Ruiz-García and Miranda 2003, 2005), the target roof displacement for a CM building can be estimated as:

$$\delta_t = C_0 C_R S_a \frac{T_e^2}{4\pi^2} g \tag{3}$$

where coefficient C_0 is described in Figure 4, S_a is the pseudo-acceleration spectral ordinate, T_e is the effective period of vibration of the building under consideration, and g is the acceleration of gravity.

INELASTIC DISPLACEMENT RATIO FOR CM BUILDINGS

The inelastic displacement ratio is defined as the maximum lateral inelastic displacement demand, Δ_i, normalized by the maximum lateral elastic displacement demand, Δ_e, of single-degree-of-freedom systems having the same mass, same first-mode period of vibration (i.e., initial stiffness), and same damping ratio when subjected to a given earthquake acceleration time-history. This ratio can be expressed as:

$$C_R = \frac{\Delta_i}{\Delta_e} \tag{4}$$

In the above equation, Δ_i is computed in systems with constant yielding strength relative to the strength required to maintain the system elastic (i.e., constant relative strength). The relative lateral strength is usually measured through the lateral strength ratio, R, defined as:

$$R = \frac{mS_a}{V_y} \tag{5}$$

where m is the mass of the system, S_a the pseudo-acceleration spectral ordinate and V_y the lateral yield strength of the system. The numerator in Equation 5 represents the lateral strength required to maintain the system elastic, which sometimes is also referred to as the elastic strength demand.

As part of this study, inelastic displacement ratios were computed from the results of time-history analyses of inelastic SDOF systems having a viscous damping ratio of 5% and six levels of R: 1.5, 2, 3, 4, 5, and 6. For each earthquake record and each level of R, twelve inelastic displacement ratios were computed to cover a period range between 0.05 and 0.5 sec, which is a representative period range for low-to-medium-height CM buildings (Muria-Vila 1990).

Regarding the hysteretic behavior used for the CM, experimental evidence gathered from in-plane cyclic testing of full-scale specimens in Mexico (e.g., Alcocer and Meli 1993, Ruiz-García 1995, Alcocer et al. 1996) has shown that CM structures exhibit significant structural degradation (i.e., stiffness degradation, strength deterioration, and pinching). Because of this, an enhanced version of the well-known *three-parameter model* (Kunnath 2003) was used in order to capture the global force-deformation response of CM structures. This analytical model is able to simulate several types of hysteretic behavior through an adequate selection of parameters that control the rate of stiffness degradation, strength deterioration, and pinching, which are function of the displacement ductility reached in previous cycles and the dissipated hysteretic energy. The parameters were calibrated using the force-deformation data obtained from a thee-dimensional full-scale two-story confined masonry specimen (designated as specimen 3-D) tested under lateral cyclic loading controlled through a displacement-based protocol (Ruiz-García 1995, Alcocer et al. 1996). A comparison of the experimental and simulated hysteretic response of specimen 3-D is shown in Figure 5. It can be seen that the hysteretic analytical model can capture the main features of the experimental hysteretic response.

The results reported herein were obtained from an ensemble of 54 earthquake ground motions recorded during nine historical earthquakes occurred in Mexico. While the earthquakes exhibited surface-wave magnitudes ranging from 5.4 to 8.0, the accelerograms were recorded on free-field stations located on firm soil sites that in turn were closely located to the subduction zone of the Mexican Pacific Coast. The data included acceleration time histories recorded during the Michoacan 1985 earthquake (M_w=8.0)

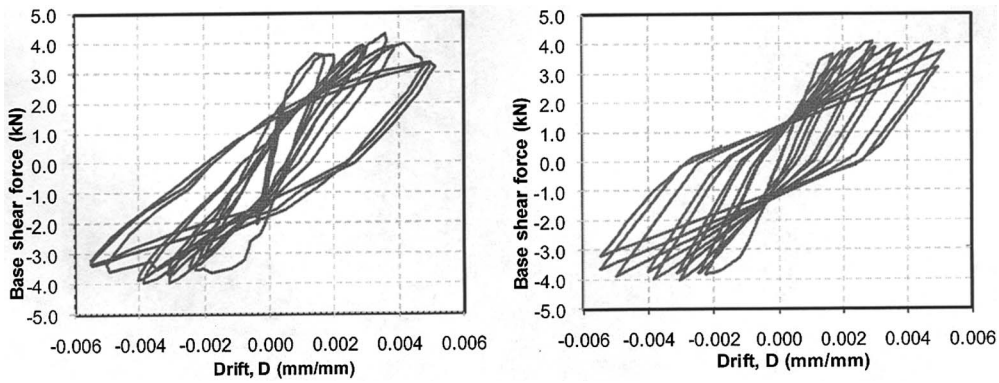

Figure 5. Simulation of the global hysteretic response of confined masonry buildings considered in this study.

and the Manzanillo 1995 earthquake (M_w=8.0). It should be noted that none of the records exhibit pulse-type characteristics or directivity effects. The sample mean of elastic pseudo-acceleration and displacement spectra computed from the ground motion ensemble are shown in Figure 6. The geometric mean of C_R obtained from all 54 records, which is a central tendency measure for this parameter, is shown in Figure 7a. In general, for the typical period range of confined masonry buildings, the central tendency of C_R strongly depends on T and R (i.e., C_R increases at a nonlinear rate as T decreases and R increases). In this period range, *the equal displacement approximation* (e.g., Veletsos et al. 1965), widely used in seismic codes to estimate maximum inelastic displacement demands, does not hold, and it could lead to significant underestimations of maximum inelastic displacement demands for CM structures. Although the C_R ordinates are different, the trend shown in Figure 7a is consistent with prior results of C_R computed from models having other structural degradation hysteretic features (Ruiz-García and Miranda

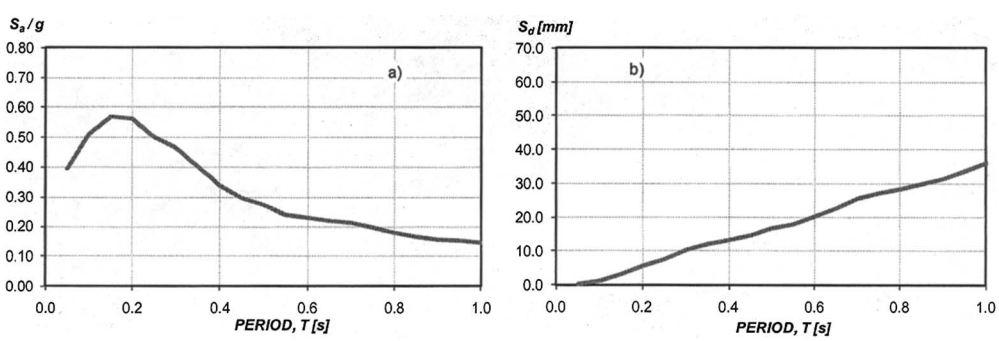

Figure 6. Central tendency of elastic spectra (ξ=0.05) obtained from the set of ground motions used in this study: a) spectral pseudo-acceleration, b) spectral displacement.

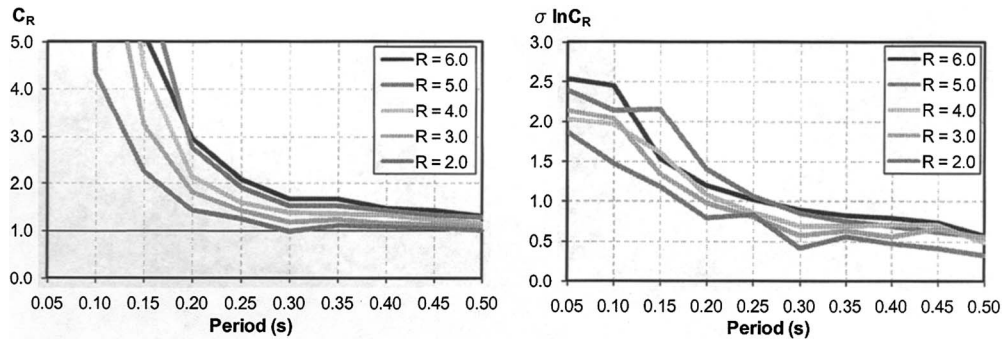

Figure 7. Statistical parameters of inelastic displacement ratios computed for systems representative of confined masonry structures: a) geometric mean; b) logarithmic standard deviation.

2005, *FEMA 440* 2005). In addition, Figure 7b shows the dispersion of C_R, expressed by the standard deviation of the natural logarithm of C_R. The high levels of dispersion in the estimation of C_R for very short period systems can be explained due to the sensitivity of the structural degrading model to some earthquake ground motions leading to a high record-to-record variability of C_R.

Simplified Equation to Estimate C_R for CM Buildings

The estimation of maximum inelastic roof drift demands for CM buildings requires a simplified equation to estimate C_R. The following equation proposed by Ruiz-García and Miranda (2003, 2005) and later incorporated into *FEMA 440* (2005) is used herein to estimate the central tendency of C_R:

$$C_R = 1 + \left(\frac{1}{a \cdot T_1^b}\right)(R - 1) \tag{6}$$

where a and b are coefficients that can be obtained from regression analysis. A nonlinear regression analysis was conducted using the subroutine **nlfit.m** as implemented in MATLAB (MathWorks 2001) to compute coefficient estimates $\hat{a}$=260 and $\hat{b}$=3 from the sample results presented in the last section. A comparison of fitted C_R using Equation 6 and the aforementioned coefficient estimates with respect to sample C_R results is shown in Figure 8. It can be seen that Equation 6 provides good estimates of the geometric mean of C_R and it is suitable to be used to obtain rapid estimates of target roof displacement using Equation 3. Note that the estimates of a and b discussed above are only applicable to buildings built of hand-made clay brick masonry walls located in the Mexican Pacific region. Specific calibration of these parameters would be required for sites that generate ground motions exhibiting significantly different dynamic characteristics and/or buildings built of other types of masonry units.

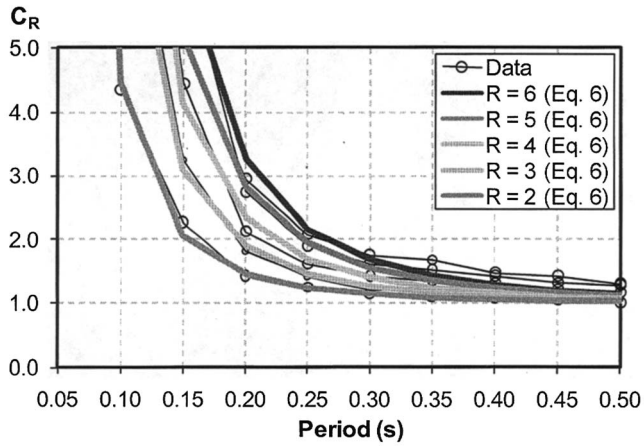

Figure 8. Comparison of central tendency (geometric mean) of inelastic displacement ratios computed in this study with those estimated from Equation 6.

SIMPLIFIED NONLINEAR ANALYSIS TECHNIQUE FOR CM BUILDINGS

As discussed in *FEMA 440* (2005), the implementation of a practical displacement-based evaluation procedure requires the development of nonlinear seismic analysis techniques that apply to the structure to be assessed. Thus, a nonlinear model capable of reflecting the inter-story and local response of CM buildings as a function of their lateral displacement demands needs to be developed. Because of its ability to model the elastic properties of walls, the aforementioned *wide-column* model represents a good starting point in the development of such a nonlinear model.

BASIS FOR A MODIFIED WIDE-COLUMN MODEL

Based on analytical and experimental research, two facts have been established: a) the wide-column model represents a feasible alternative for modeling the elastic behavior of CM walls (e.g., Bazán 1980, San Bartolome 1994, Zuniga and Terán-Gilmore 2008); and b) the lateral response of CM walls is governed by shear deformations, particularly as the walls experience increasing inelastic behavior (e.g., Alcocer and Meli 1993, San Bartolome 1994). Based on these facts, a modified version of the wide-column model, which exclusively relates the lateral stiffness degradation of the CM wall to its shear properties, can be formulated. This assumption implies that after the diagonal cracking in the wall's surface occurs, the flexural stiffness component remains constant while the shear stiffness component is modified as a function of the drift demand. According to this, the lateral stiffness of a CM wall can be established as a function of its lateral deformation:

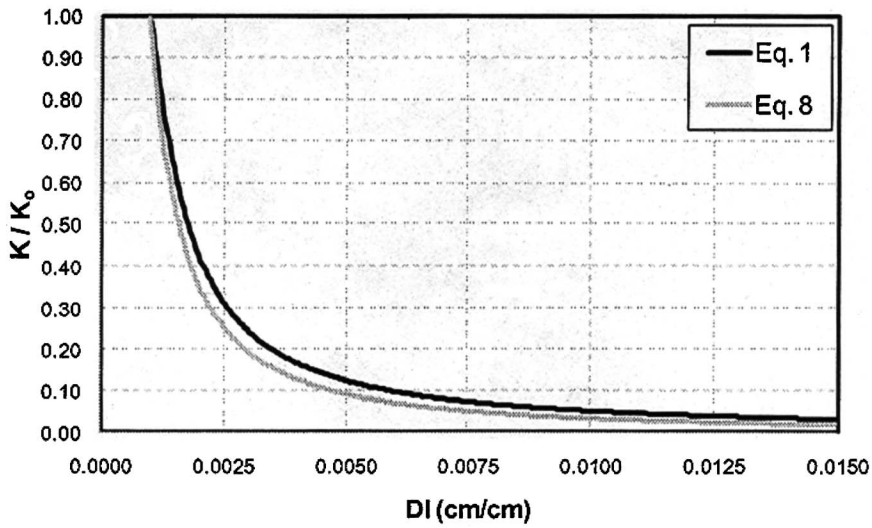

Figure 9. Stiffness degradation according to Equations 1 and 8.

$$K = \left[\frac{h^3}{\beta EI} + \frac{h}{GA \cdot (k_i/k_o)_s} \right]^{-1} \tag{7}$$

where K is the total lateral stiffness; and $(k_i/k_o)_s$ is the stiffness degradation index due to shear deformation.

To evaluate the pertinence of using the modified *wide-column* model for nonlinear analysis, this model was used to establish shear stiffness degradation curves for the *W-W*, *WBW*, *WWW* and 3-D specimens (Alcocer and Meli 1993, Ruiz-García 1995, Alcocer et al. 1996). Since all four specimens had two-coupled, it was considered that the shear properties of each wall were degraded in the same proportion during the estimation of the curves. From nonlinear regression analysis, the following expression was adjusted to the D_i versus $(k_i/k_o)_s$ curves obtained for the different specimens:

$$\left(\frac{k_i}{k_o} \right)_S = \frac{D_i^{-1.46}}{25000} \leqslant 1.0 \tag{8}$$

where $(k_i/k_o)_S$ is the shear stiffness degradation factor corresponding to D_i; and D_i an inter-story drift corresponding to inelastic behavior.

Figure 9 compares the stiffness degradation curves established from Equations 1 and 8. Note that while Equation 1 establishes a relation between the total lateral stiffness and the total elastic lateral stiffness measured experimentally in CM specimens, Equation 8 offers a similar relation for the shear lateral stiffness. Because both curves compare reasonably well, it can be concluded that: a) The degradation of the structural properties of a CM wall is fundamentally associated to its shear behavior; and b) a modified *wide-*

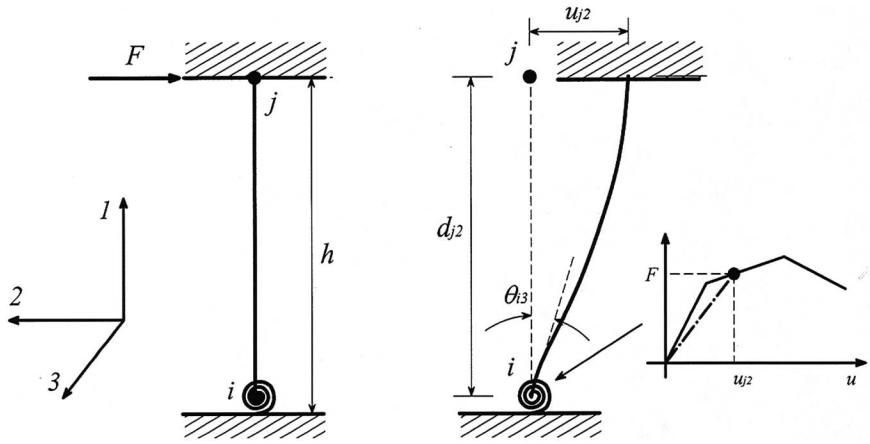

Figure 10. Modified wide-column model for static nonlinear analysis.

column model offers reasonable nonlinear modeling for low-height masonry buildings. It should be emphasized that the k_i/k_o ratios included in Equations 1 and 8 were used to validate the proposed nonlinear model, and that they do not form part of the assessment procedure discussed herein.

NONLINEAR STATIC ANALYSIS PROCEDURE FOR CM BUILDINGS

The nonlinear analysis of moment-resisting frames usually considers that inelastic behavior concentrates in plastic hinges located at the ends of beams and columns. Usually, shear deformations on these structural elements are neglected, in such manner that only flexural properties need to be modeled. Contrasting with this situation, the shear effects on masonry walls are important and should be explicitly considered. Nonlinear analysis of earthquake-resistant structures needs to account for two types of nonlinearity; the first related to the material's behavior and the second to the deformed configuration of the structure. In the case of low-height CM buildings, the displacement threshold associated to ultimate is usually low, in such manner that the second type of nonlinearity can be neglected.

The model proposed herein to make possible a pushover analysis of a CM building implies modeling each wall through a modified *wide-column*. While the flexural stiffness of the walls is kept constant during the analysis, their shear properties are modified according to the Flores and Alcocer (1996) backbone curve (see Figure 2). Figure 10 illustrates the modified *wide-column* model technique: while a constant flexural stiffness is assigned to the column, the shear behavior of the wall (including its inelastic range of behavior) is modeled through a rotational spring located at its base having a force-deformation relationship defined by the backbone illustrated in Figure 2. The spring is located at the base with the purpose of relating the inelastic shear behavior of the walls with the inter-story drift due to shear deformation. Figure 11a shows specimen 3-D modeled through the modified *wide-column* modeling technique using the commercial

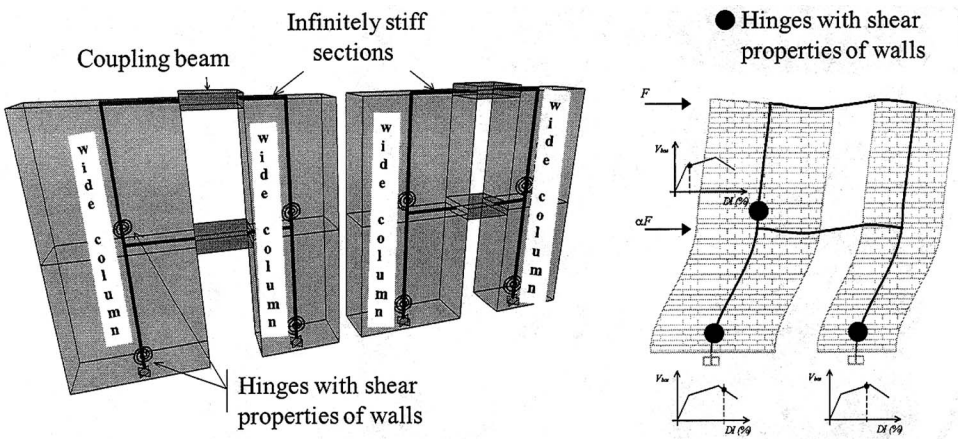

Figure 11. Modified wide-column model for Specimen 3-D: a) Nonlinear model, and b) damage assessment.

software *SAP2000* (Computers and Structures Inc. 2004). In addition, Figure 11b shows the deformed shape and potential plastic hinges in specimen 3-D under increased lateral displacement.

A comparison of the base shear-lateral drift envelope curves (positive in dark gray lines and negative in light gray lines) obtained experimentally from the referenced confined masonry specimens (W-W, WBW, WWW and 3-D) with the capacity curves (in black lines) derived from the proposed pushover analysis technique is shown in Figures 12a–12d. In spite of the high variability observed in the experimental curves, the modeling technique proposed herein yields reasonable conservative estimates of the capacity curves. Note that the initial elastic stiffness as well as the lateral force associated to first cracking is estimated with high precision. Besides providing a reasonable estimate of global behavior, the modeling technique allows for a reasonable estimation of the evolution of structural damage at the local level. This is illustrated in Figure 11b for specimen 3-D, which accumulated in the laboratory severe damage in the walls of the ground story and light damage in one of the walls of the upper story (Ruiz-García 1995, Alcocer et al. 1996).

ILLUSTRATIVE EXAMPLE

The structural performance of a three-story CM building was evaluated using the proposed displacement-based procedure. Figure 13 shows the structural layout of a 1:2 scale model (of the building under consideration) tested at the shaking table facility located at the Institute of Engineering of National Autonomous University of Mexico, II-UNAM (Arias 2005, Barragan and Alcocer 2006). According to its physical, geometrical and mechanical characteristics, the building can be considered representative of residential buildings built in Mexico.

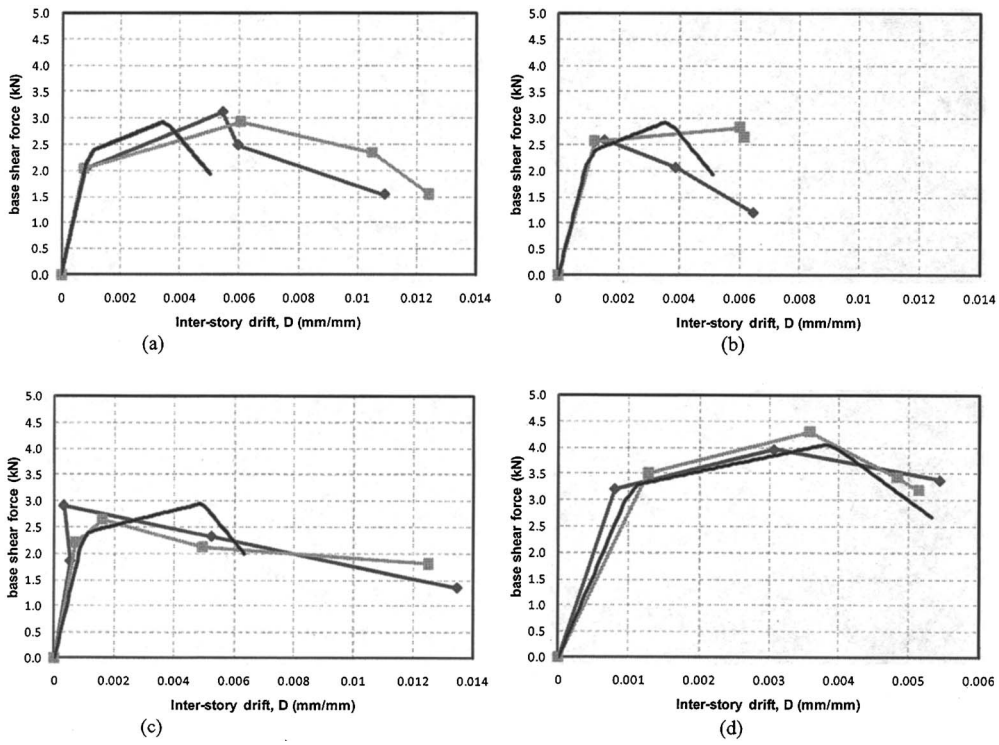

Figure 12. Comparison of capacity curves obtained experimentally and with the proposed technique for four full-scale specimens (Alcocer and Meli 1993, Alcocer et al. 1996): a) *W-W*, b) *WBW*, c) *WWW*, d) 3-D.

The design strength for the concrete used to build the tie-end elements and slab was 20 MPa; that of the mortar was established at 12.5 MPa. While #3 steel bars with a nominal strength of 420 MPa were used for the longitudinal reinforcement used in the slab and tie-end elements, the transverse reinforcement consisted in #2 stirrups built of steel having 250 MPa nominal strength. The building was designed according to the 2004 edition of the Masonry Technical Requirements of the MCBC, and has a total weight of 1060 kN. While 30.6% of this weight is located at the roof, each one of the first two stories contributes 34.7% to the total weight. A detailed description of the physical, geometrical and mechanical characteristics of the building and its 1:2 scale model (denoted specimen from here on) can be found in Arias (2005) as well as Barragan and Alcocer (2006).

The mechanical and geometrical properties of the specimen were established following rules of *simple similarity* (Arias 2005). A simple similarity model is built with materials having the same strength and weight as those used in the building it models. Table 5 summarizes the scale factors that need to be used to establish complete and simple

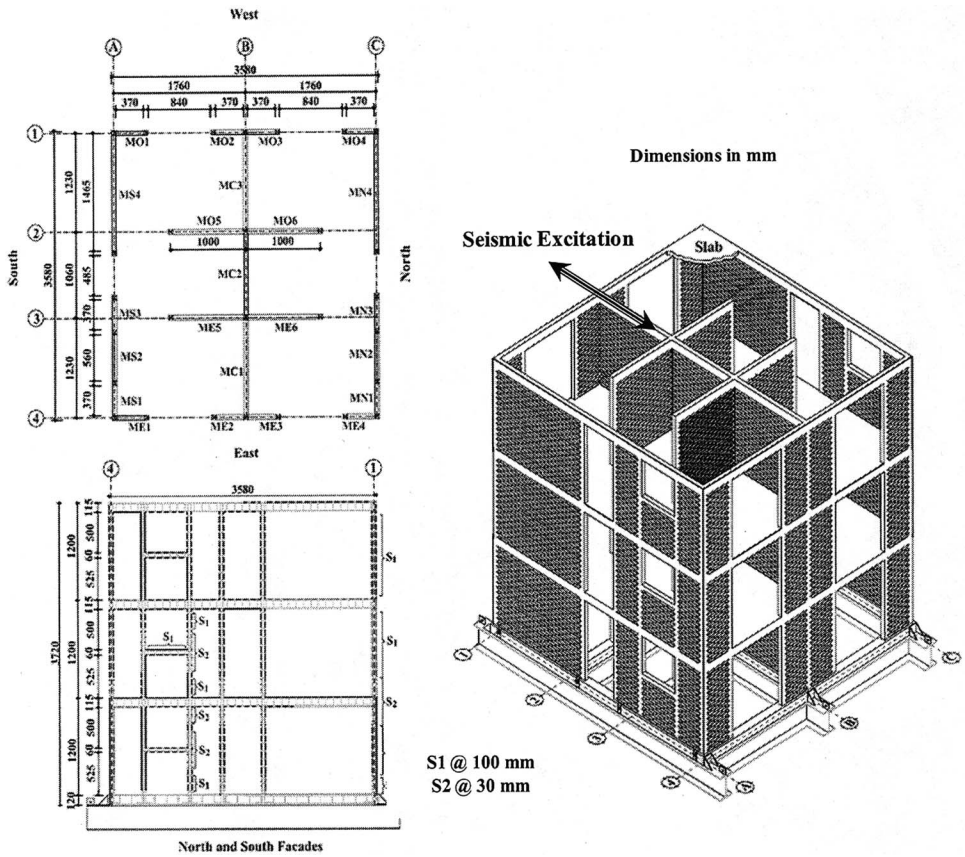

Figure 13. Structural layout of 1:2 scale model of sample confined masonry building (Barragan and Alcocer 2006).

similarities. Subscripts B and M refer to the building and its model, respectively. Note that for a 1:2 scale model, S_L equals 2.

An earthquake ground motion recorded in the Mexican Pacific coast was used as a basis for the testing program. The seed motion, recorded in the city of Acapulco, on the 25th of April of 1989, had a peak ground acceleration of 0.34 g and was recorded during a seismic event with surface-wave magnitude of 6.9. The specimen was subjected to a sequence of eight synthetic seismic excitations by increasing gradually the intensity of motion at each test run up until the maximum lateral strength of the specimen was attained. While Figure 13 indicates the direction in which the motions were applied to the specimen, Table 6 summarizes some of their characteristics and outlines the level of damage observed after the third and eighth motions.

Table 5. Scale factors for models subjected to dynamic loads (after Arias 2005)

Parameter	Equation	Complete Similitude	Simple Similitude
Length (L)	$S_L = L_B / L_M$	S_L	S_L
Strain (ε)	$S_\varepsilon = \varepsilon_B / \varepsilon_M$	1	1
Strength (f)	$S_f = f_B / f_M$	S_L	1
Stress (σ)	$S_\sigma = f_B / f_M$	S_L	1
Modulus of Elasticity (E)	$S_E = S_\sigma / S_\mathrm{E}$	S_L	1
Specific Weight (γ)	$S_\gamma = \gamma_p / \gamma_m$	1	1
Force (F)	$S_F = S_L^2 S_f$	S_L^3	S_L^2
Time (t)	$S_t = S_L (S_\gamma S_\varepsilon / S_f)^{1/2}$	$S_L^{1/2}$	SL
Frequency (ω)	$S_\omega = 1 / S_t$	$1 / S_L^{1/2}$	$1 / S_L$
Displacement (δ)	$(S_\delta = S_L S_\varepsilon)$	S_L	S_L
Acceleration (a	$S_a = S_f / (S_L S_\gamma)$	1	$1 / S_L$
Mass ($m\omega$	$S_m = S_\gamma S_L^3$	S_L^3	S_L^3
Damping (ξ)	$S_\xi = \xi_p / \xi_m$	1	1

PROPERTIES OF THE BUILDING

The properties of the modified *wide-columns* that represent each one of the walls in the building were established according to the Masonry Technical Requirements of the MCBC (2004). Figure 14 shows the spatial model used to carry out the pushover analysis of the building. The reinforced concrete slabs were considered to be infinitely rigid in-plane.

The analytical model estimates a fundamental period of vibration of 0.12 seconds. Ambient tests carried on the specimen yielded a fundamental period of vibration of 0.075 seconds, which according to the rules of simple similarity corresponds to an uncracked period of 0.15 seconds for the building. It should be mentioned that minor

Table 6. Motions used during experimental testing of 1:2 scale model

Motion	Magnitude	PGA (g)	Duration (sec)	Observations
1	7.6	1.49	15.9	
2	7.8	1.66	24.2	
3	8.0 (60%)	1.54	29.3	First significant cracking. Level of damage is associated to elastic limit (immediate operation)
4	8.3 (60%)	1.89	39.1	
5	8.0 (90%)	1.69	29.3	
6	8.3(90%)	1.97	39.3	
7	8.3(100%)	2.07	29.6	
8	8.3(125%)	2.00	39.4	The building was considered to reach its maximum lateral strength. Level of damage is associated to life safety

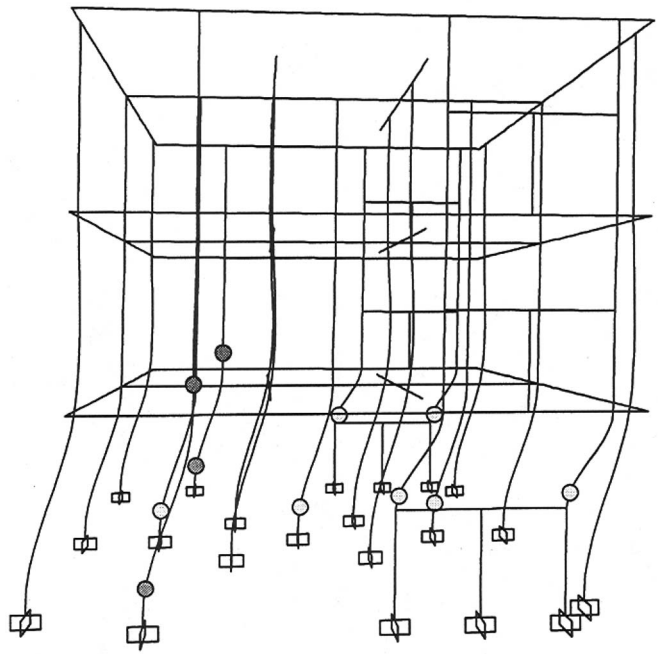

Figure 14. Analytical model of sample building.

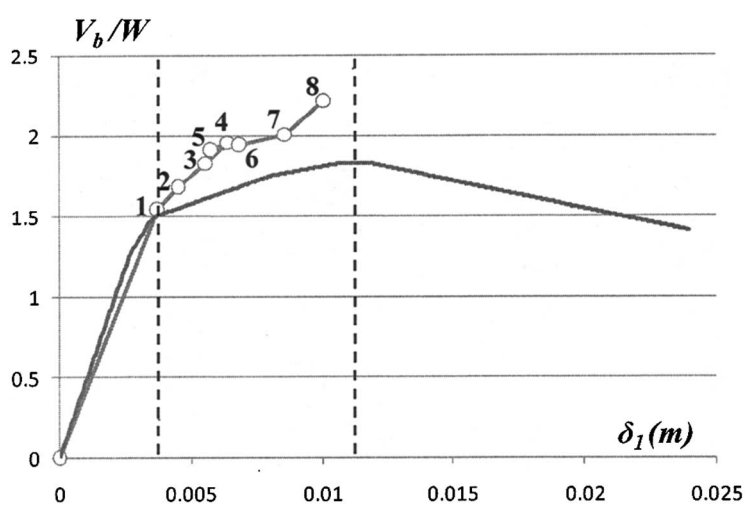

Figure 15. Capacity curves for the first story of the sample building.

cracking occurred in the specimen while it was accidentally dropped during placement (Arias 2005). Although the specimen was repaired through epoxy injection, this repair technique cannot fully restore the original stiffness of cracked walls.

Figure 15 shows with continuous line the capacity curve for the first story of the building. The curve was established by applying to the wide-column model, through a pushover analysis, a lateral load distribution proportional to that derived from a modal spectral analysis. Note in the figure that the base shear force has been normalized by the total weight of the building. The circles in the figure represent the largest lateral displacements demands and their corresponding normalized base shears derived from the experimental study of the specimen. The number associated to each circle corresponds to each one of the eight motions under consideration. While the lateral displacements obtained directly from the specimen were scaled up by a factor of two, the normalized base shear is a dimensionless parameter that does not require scaling.

The "analytical" and "experimental" curves exhibit a good correspondence. The vertical discontinuous lines included in Figure 15 establish the displacement thresholds that according to the analytical model can be associated to first significant cracking (immediate operation) and maximum lateral strength (life safety). The lateral displacement that according to the experimental evidence is associated to the maximum lateral strength of the building (eighth motion) has a close correspondence with its analytical counterpart. Although the specimen shows a noticeable softening after the first motion, significant cracking was first observed after the third motion. A fair correspondence can be observed between the experimental and analytical thresholds for first significant cracking. While a good coincidence for the initial stiffness predicted by both curves is observed, the main difference involves a larger post-cracking stiffness for the experimental derived curve.

ROOF DISPLACEMENT

To establish estimates of roof displacements demands (δ_t) for the analytical model, first it is necessary to establish within its capacity curve the base shear associated to first yielding (V_y). Although a CM building does not strictly "yield', it is reasonable to consider first cracking as the yielding point for the building. By using Figure 15, it is possible to establish that V_y/W equals 1.5. The effective fundamental period of the building (denoted T_e in Figure 4) is equal to its elastic fundamental period (T_i); that is, T_e is equal to 0.12 seconds. With the values of V_y/W and T_e under consideration, roof displacement demands for the building were estimated with Equations 3, 5, and 6 for a wide range of values of S_a/g. As shown in Figure 16, the displacement demands increase linearly up to a value of 1.5. After that, they increase at a higher rate as the value of S_a/g increases beyond that threshold. Note that the figure includes two curves, one corresponding to C_o equal to 1.2, and a second one for C_o of 1.0.

Figure 17 shows elastic strength spectra corresponding to the third and eighth motions included in Table 6. The spectra correspond to 5% of critical damping. As required by simple similarity, the motions recorded at the shake table were scaled up by two in terms of time and scaled down by two in terms of acceleration. For a period of 0.12 seconds, S_a/g demands of 2.0 and 2.4 correspond to the third and eighth motions,

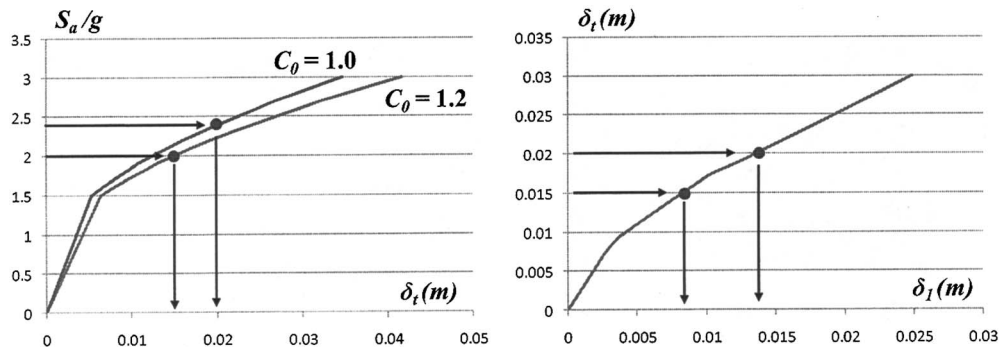

Figure 16. Lateral displacement demands on sample building: a) Roof, and b) First story.

respectively. According to the levels of damage observed in the specimen, values of 1.2 and 1.0 should be assigned to C_o for the evaluation of δ_t, respectively (see Tables 4 and 6). The estimation of δ_t (illustrated in Figure 16a) results in roof displacement demands of 0.015 and 0.020 meters, respectively. Experimental roof drift ratios of 0.00233 and 0.00333 were estimated for the specimen for these motions. To obtain experimental roof estimates for the building, these values need to be multiplied by the total height of the specimen (3.60 m) and then, to achieve similarity, scaled up by two. According to this, experimental roof displacements of 0.017 and 0.024 meters, respectively, are obtained.

To assess the level of damage in the critical story, the methodology requires the estimation of inter-story drift ratios. According to the pushover analysis, roof displacements of 0.015 and 0.020 meters correspond to first floor displacements (δ_1) of 0.008 and 0.013 meters, respectively (see Figure 16b). For a story height of 2.40 meters, this implies inter-story drift ratios of 0.0033 and 0.0054, respectively. Experimental inter-story drift ratios for the first story of the specimen are 0.0023 and 0.0042 (no scaling is required because of the dimensionless nature of this parameter). Figure 18 illustrates

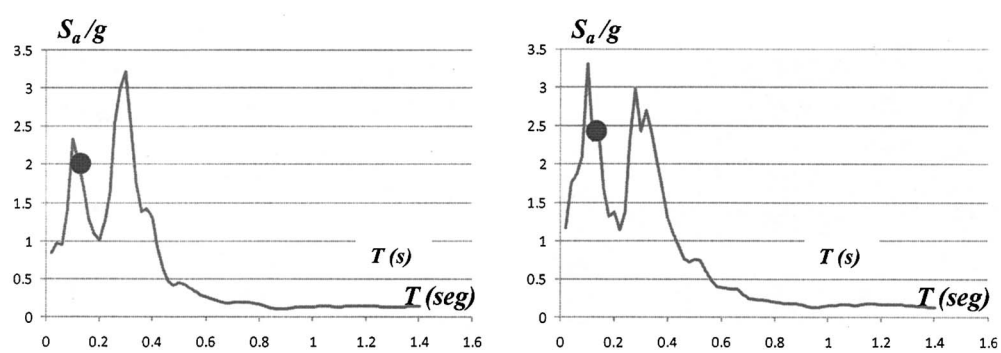

Figure 17. Elastic strength spectra corresponding to motions three and eight.

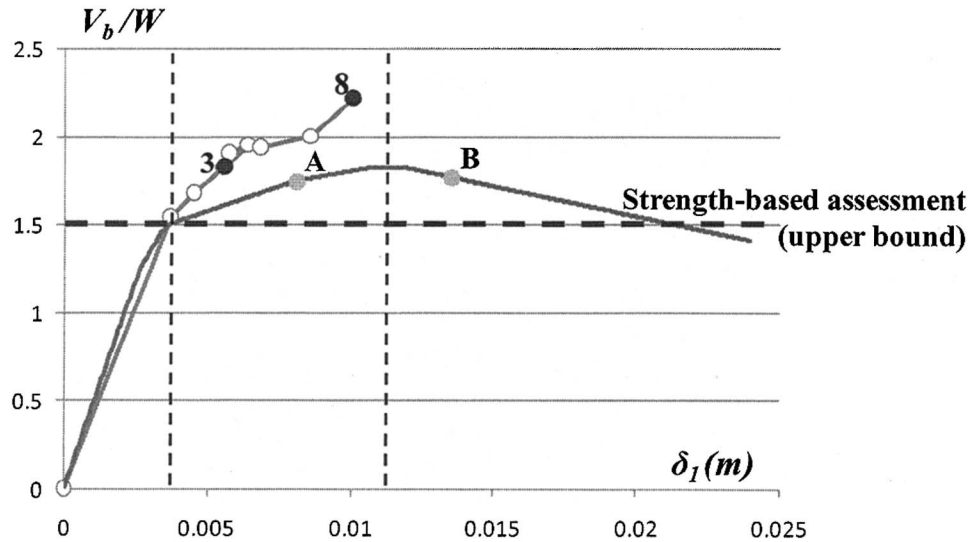

Figure 18. Performance assessments for sample building.

analytical and experimental displacement demands in the first story (points A and B correspond to analytical demands for the third and eighth motions, respectively). Using the recommendations included in Table 1, the proposed methodology establishes a damage level *Heavy-V* for the third motion, and damage level *Severe* (close to ultimate) for the eighth motion. According to the descriptions provided by Arias (2005), damage in the specimen's walls for these motions correspond to *Moderate-III* and *Heavy-V*, respectively. While Figure 19 shows the crack patterns exhibited by the specimen after the eighth motion, Figure 14 indicates with circles the walls that according to the proposed methodology exhibit nonlinear behavior for that motion. Both the experimental and analytical models indicate that damage tends to concentrate in the first story, and that a few walls in the second story end up slightly damaged.

The proposed methodology yields conservative assessment of damage for the sample building. On one hand, the recommendations given in Table 1 (derived from pseudo-static cyclic testing of CM walls) are conservative when applied to walls subjected to dynamic loading. For instance, while the table indicates that a pseudo-statically applied drift of 0.0013 results in first diagonal cracking in the wall's surface, the measurements derived from the shaking table indicate first cracking occurs at drifts larger than 0.0020. On the other hand and for similar reasons, the Flores and Alcocer (1996) model used to formulate the wide-column nonlinear model predicts that cracking occurs at smaller drifts than those observed experimentally in the shaking table. Because of this, the nonlinear model predicts the formation of the soft first story earlier than it should; and as a consequence, the first story inter-story drifts predicted by the proposed procedure are larger than those measured experimentally.

Before concluding this section, the authors would like to discuss three issues:

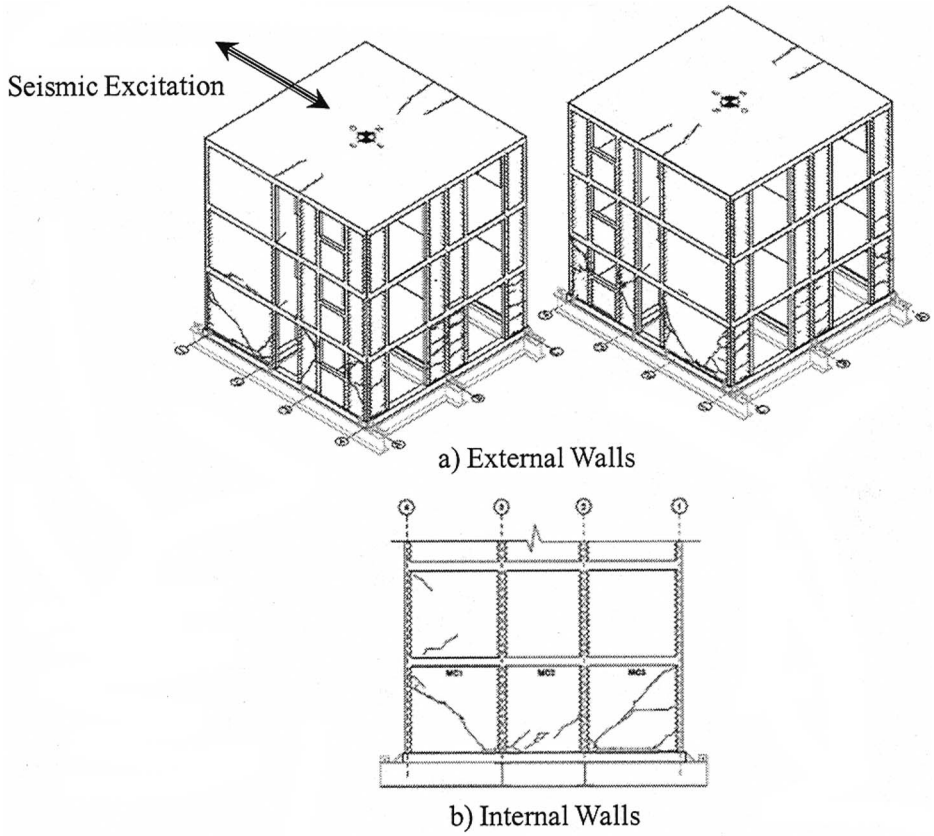

Figure 19. Damage on 1:2 scale model after eighth motion (Arias 2005, Barragan and Alcocer 2006).

1. Strictly speaking, the methodology introduced herein should not have been used to predict the displacement demands corresponding to the eighth motion included in Table 6. While the methodology assumes the building is undamaged before the motion, the specimen was moderately damaged before the eighth motion was applied to it. Nevertheless, as discussed in detail in FEMA-273/274 (1997), previous damage of moderate nature usually is reflected in large differences in displacement demands for low intensity motions. Displacement demands in the damaged and undamaged states of a building would tend to be similar for high intensity motions (the authors believe that this is the case for the sample building subjected to the eighth motion).
2. The advantages of using displacement-based assessment over force-based assessment can be discussed through the sample building. From a strength perspective, an upper bound base shear for the building can be estimated by adding up the shear strength, estimated according to the Masonry Technical Require-

ments of the MCBC (2004), of all the walls located in the first story. As Figure 18 shows, the force-based normalized base shear (V_y/W) is equal to 1.5 (this estimate does not include a 0.7 strength reduction factor, which strictly speaking and according to the MCBC, should be considered during the strength evaluation). An "optimistic" force-based assessment of the sample building indicates that a spectral ordinate S_a/g greater than 1.5 requires the seismic rehabilitation of the building. Nevertheless, the displacement-based assessment shows that the building can accommodate values of S_a/g close to 2.4 before reaching its ultimate capacity. In spite of its conservative nature, the displacement-based assessment predicts that the building exhibits 60% more seismic capacity with respect to the most optimistic force-based assessment.

3. An alternative for estimating the roof displacement demand in a building is the use of a simplified SDOF dynamic analysis as suggested in FEMA273/274 (1997) and subsequent FEMA documents. Within this context, an equivalent SDOF system having hysteretic behavior illustrated in Figure 5 should be established from the capacity curve of the CM building as discussed in (Zuñiga and Terán-Gilmore 2008).

CONCLUSIONS

Displacement-based assessment methodologies can and should be formulated for confined masonry buildings. In the case of low-height confined masonry buildings, their dynamic behavior is dominated by their fundamental mode of vibration, in such manner that the *coefficient method* can be adapted to provide reasonable estimates of their local and global lateral deformation demands. Furthermore, the degradation of the structural properties of the walls is fundamentally associated to their shear behavior, in such a manner that a simplified nonlinear model derived from the widely used *wide-column* model is able to provide a reasonable estimate of the capacity curve of such buildings. The integration of the coefficient method and the simplified nonlinear model constitutes the basis from which a simple and reliable displacement-based assessment methodology for low-height confined masonry buildings can be formulated.

The application of the proposed displacement-based procedure to a three-story building yielded reliable estimates of its global and local deformation demands. The demands predicted by the methodology have a close correspondence to those estimated for the same building from the measurements taken on a 1:2 scale model tested on a shaking table. Regarding the estimation of the level of damage and structural degradation in the walls, the methodology yields conservative estimates for the damage observed during the experimental studies.

Displacement-based assessment procedures provide an adequate understanding of the response of confined masonry buildings to seismic ground motions of different intensity. While force-based procedures tend to underestimate the seismic capacity of a structure and does not provide an understanding of how to achieve certain performance levels, displacement-based procedures are capable of better estimating the actual capacity of the building, and to provide useful insights into what does an engineer need to do so that a particular building can achieve adequate damage control. The application of

displacement-based assessment procedures has the potential to produce efficient and reliable design of confined masonry structures located in zones of high seismic hazard.

Although the proposed procedure allow for an estimation of inelastic displacement demands during the seismic assessment of masonry buildings, the information that is currently available does not cover numerous situations that can occur in real confined masonry buildings. Therefore, it is necessary to carry out further studies targeted at developing and integrating experimental, analytical and field data to allow for a better calibration of the seismic assessment procedure proposed herein.

ACKNOWLEDGMENTS

While the first and second authors would like to express their gratitude to Universidad Autónoma Metropolitana, the third author wishes to thank Universidad Michoacana de San Nicolás de Hidalgo in México for the support provided to develop the research reported in this paper. The authors would also like to express their recognition to the research carried out by Prof. Sergio M. Alcocer (Institute of Engineering at UNAM) and his research associates, and thank them for sharing their experimental data and some of the figures included in this paper. Finally, special thanks to the responsible editor and three anonymous reviewers, whose observations were instrumental in improving the original version of the paper.

REFERENCES

Alcocer, S. M., and Meli, R., 1993. Test program on the seismic behavior of confined masonry walls, *Masonry Soc. J.* **13**, 68–76.

Alcocer, S. A., Ruiz, J., Pineda, J., and Zepeda, J. A., 1996. Retrofitting of confined masonry walls with wire-welded mesh, *Proceedings of the Eleventh World Conference on Earthquake Engineering*, Acapulco, Paper No. 1471.

Applied Technology Council (ATC), 1996. *Seismic evaluation and retrofit of concrete buildings*, *Report ATC-40*, Redwood City, CA.

Arias, J., 2005. Shaking-table tests of a 1:2 scale three-story confined masonry building model (in Spanish), M.E. thesis, National University of Mexico.

Barragan, R., and Alcocer, S. M., 2006. Shaking table tests on half-scale models of confined masonry made of handmade solid clay bricks, in *Proceedings of the First European Conference on Earthquake Engineering and Seismology*, Geneva, Paper No. 1147.

Bazán, E., 1980. Masonry walls under lateral loading: Analytical studies, Ph.D. thesis, National University of Mexico.

Calvi, G. M., 1999. A displacement-based approach for vulnerability evaluation of classes of buildings, *J. Earthquake Eng.* **3**, 411–438.

Computers and Structures, Inc., 2004. *SAP2000 Advanced 9.0.3*, Berkeley, California.

Earthquake Engineering Research Institute (EERI), 2006. *The Tecoman, Mexico, Earthquake, January 21, 2003*, EERI-SMIS Reconnaissance Report.

Federal Emergency Management Agency (*FEMA 273/274*), 1997. *Prestandard and commentary for the seismic rehabilitation of buildings*, *Report FEMA 273/274*, Washington, D.C.

Federal Emergency Management Agency (*FEMA 306*), 1999. *Evaluation of earthquake damaged concrete and masonry wall buildings*, *Report FEMA 306*, Washington D.C.

Federal Emergency Management Agency (*FEMA 356*), 2000. *Prestandard and commentary for the seismic rehabilitation of buildings*, *Report FEMA 356*, Washington D.C.

Federal Emergency Management Agency (*FEMA 440*), 2005. *Improvement of nonlinear static seismic analysis procedures*, *Report FEMA 440*, Washington D.C.

Flores, L., and Alcocer, S. M., 1996. Calculated response of confined masonry structures, in *Proceedings of the Eleventh World Conference on Earthquake Engineering*, Acapulco; Paper No. 1830.

Kunnath, S. K., 2003. *IDASS: Inelastic Dynamic Analysis of Structural Systems, Version 3.01*, University of California at Davis, CA.

MathWorks Inc., 2001. *MATLAB, Version 6.1*, The MathWorks Inc., Natick, MA.

Mexico City Building Code (MCBC), 2004. *Normas Técnicas Complementarias para Diseño y Construcción de Estructuras de Mampostería*, Gaceta oficial, Gobierno del Distrito Federal (in Spanish).

Muria-Vila, D., 1990. Dynamic behavior of masonry buildings in Mexico City, in *Proceedings of the Fifth North American Masonry Conference*, Univ. of Illinois at Urbana-Champaign; Vol I: 127–138.

Rodríguez, M., 2005. Design and evaluation of masonry dwellings in seismic zones, *Earthquake Spectra* **21**, 465–492.

Ruiz-García, J., 1995. Retroffiting of a full-scale two-story tri-dimensional confined masonry structure (in Spanish), M.E. thesis, National University of Mexico.

Ruiz-García, J., and Alcocer, S. M., 1998. Experimental performance of confined masonry structures retrofitted with welded wire mesh (in Spanish), *Revista de Ingeniería Sísmica* **59**, 59–79.

Ruiz-García, J., Sánchez, T., and Miranda, E., 2003. Chapter 6: Observations of the behavior and design of masonry dwellings in seismic zones (in Spanish), in *Edificaciones de mamposteíia para vivienda*, Fundación ICA-SMIE.

Ruiz-García, J., and Miranda, E., 2003. Inelastic displacement ratios for evaluation of existing structures, *Earthquake Eng. Struct. Dyn.* **32**, 1237–1258.

Ruiz-García, J., and Miranda, E., 2005. Performance-based assessment of existing structures accounting for residual displacements, *Report TR-153*, The John A. Blume Earthquake Engineering Center, Stanford University, Palo Alto, CA, http://blume.stanford.edu/Blume/TechnicalReports.htm.

San Bartolome, A., 1994. *Masonry Construction, Seismic Behavior, and Structural Design* (in Spanish). Pontificia Universidad Católica del Perú, Fondo Editorial; 228 pp.

Veletsos, A. S., Newmark, N. M., and Chelapati, C. V., 1965. Deformation spectra for elastic and elastoplastic systems subjected to ground shock and earthquake motions, in *Proceedings of the Third World Conference on Earthquake Engineering*, Vol. II, New Zealand, 663–682.

Zuñiga, O., and Terán-Gilmore, A., 2008. Displacement-based evaluation of confined masonry buildings (in Spanish), *Revista de Ingeniería Sísmica*, Sociedad Mexicana de Ingeniería Sísmica **79**, 25–48.

(Received 12 March 2008; accepted 10 December 2008)